Food Chemistry 460 (2024) 140694

Contents lists available at ScienceDirect

Food Chemistry

journal homepage: www.elsevier.com/locate/foodchem

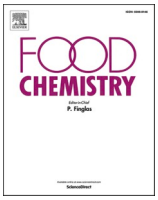

Production and simulated digestion of high-load beads containing *Schizochytrium* oil encapsulated utilizing prilling technique

Gabriele Beltrame [a], Annelie Damerau [a], Eija Ahonen [a], Sari A. Mustonen [a], Renata Adami [b], Maria Rosaria Sellitto [c], Pasquale Del Gaudio [c,d,**,1], Kaisa M. Linderborg [a,*,1]

[a] Food Sciences, Department of Life Technologies, University of Turku, FI-20014 Turku, Finland
[b] Department of Physics, University of Salerno, IT-84084 Fisciano, Italy
[c] Department of Pharmacy, University of Salerno, IT-84084 Fisciano, Italy
[d] Research Centre for Biomaterials BIONAM, University of Salerno, IT-84084 Fisciano, Italy

ARTICLE INFO

Keywords:
Schizochytrium
Prilling
Alginate
Lipid oxidation
Simulated digestion
DHA

ABSTRACT

The oil from the heterotroph *Schizochytrium* is a rich source of n-3 PUFA, particularly DHA, and therefore highly susceptible to oxidation. The present work reports the first application of coaxial prilling for the protection of this oil through microencapsulation. After process optimization, core-shell microparticles were produced with calcium or zinc alginate at different concentrations. Encapsulates were analyzed in their tocopherol and PUFA content. Prilling lowered the earlier but had little effect on the latter. Microcapsules coated with calcium alginate (1 % and 1.75 %) had higher oil load and encapsulation efficiency and were therefore submitted to *in vitro* digestion together with a simulated meal. Digesta were also analyzed with HPLC-qTOF and ^{1}H NMR and compared to undigested encapsulates. While 1 % calcium shell granted lower oil release and protection from oxidation in the simulated gastrointestinal tract, chromatographic and spectroscopic data of digesta showed higher presence of lipid digestion products.

1. Introduction

Polyunsaturated fatty acids (PUFAs), in particular docosahexaenoic acid (C22:6n-3, DHA) and eicosapentaenoic acid (C20:5n-3, EPA) play an essential role in human well-being at all development stages. PUFAs are involved in the homeostasis of inflammation response, platelet aggregation, vasodilation, eyesight, and bone integrity. They provide protection against disorders such as cardiovascular diseases and osteoporosis (Saini & Keum, 2018). Despite their importance, the dietary intake of omega-3 PUFAs has been found lower than the FAO and EFSA recommendations in 81 % of the world population (Micha et al., 2014).

Fish is the primary source of DHA and EPA in the human diet. However, the world fish industry can address only 30 % of the human population omega-3 requirement (Hamilton et al., 2020). Capture fisheries around the world are at or beyond sustainability level, and although aquaculture has relieved some pressure from wild fish stocks, it still requires external sources of PUFAs (Tocher, 2015). In addition, the global stock of DHA is expected to decline with the projected increase of water temperature (Colombo et al., 2020). Therefore, new omega-3 needs to be generated outside the current system to fill the gap between supply and demand. The primary producers of DHA and EPA, i.e. marine microorganisms cultivated in bioreactors, would be a sustainable alternative for production of oil rich in PUFAs. Marine traustochytrids such as *Schizochytrium* sp. have multiple advantages compared to proper microalgae: lower energy requirements due to their heterotrophic metabolism, cellular lipid content of over 70 %, high amounts of DHA esterified in triacylglycerols. Oil extracted from *Schizochytrium* sp is already utilized commercially and currently dominates the market of vegan omega-3 supplements (Demets & Foubert, 2021).

Despite its suitability for vegetarian and vegan diets, the organoleptic properties of oils, including *Schizochytrium* sp, are challenging for most consumers. Oils with high PUFA content are prone to oxidation due to their high degree of unsaturation. Oxidation of omega-3 yields a multitude of products (aldehyde, ketones, epoxides, oxo-fatty acids) which not only cause the formation of unpleasant flavor but also decrease the nutritional quality of PUFAs. Some oxidations products are

* Correspondence to: Kaisa M. Linderborg, Food Sciences Unit, Department of Life Technologies, University of Turku, FI-20014 Turku, Finland.
** Correspondence to: Pasquale Del Gaudio, Department of Pharmacy, University of Salerno, I-84084 Fisciano, Italy.
E-mail addresses: pdelgaudio@unisa.it (P. Del Gaudio), kaisa.linderborg@utu.fi (K.M. Linderborg).
[1] These authors contributed equally to this work.

https://doi.org/10.1016/j.foodchem.2024.140694
Received 4 March 2024; Received in revised form 1 July 2024; Accepted 27 July 2024
Available online 2 August 2024

bioactive, and thus of physiological importance (Serini et al., 2011). These setbacks can be addressed with oil encapsulation. This is an effective and widely applied technology for the protection of PUFAs from oxygen and pro-oxidants and masking of unpleasant flavors. Different omega-3-rich oils have been encapsulated utilizing different wall materials such as maltodextrins, starch, whey protein, and gelatin (Schwarz & Amft, 2021). For example, Baltic herring oil has been encapsulated with a blend of rice and whey protein with maltodextrin (Damerau, Ogrodowska, et al., 2022), krill oil with gum arabic (Ortiz Sánchez et al., 2021), and shrimp oil with a blend of whey protein, casein, and maltodextrin (Takeungwongtrakul et al., 2015).

One of the emerging and promising strategies for encapsulating sensitive substances is the prilling technique, also known as laminar jet break-up. This easy to scale-up technology allows the controlled formation of either soft or hard gel beads by using a vibration-assisted extrusion. The process involves the breaking of a polymeric feed solution into drops with vibrating nozzle and their subsequent gelation into a collection solution (Del Gaudio et al., 2005). The application of the proper frequency either on the vibrating nozzle or on the liquid ensures the formation of monodispersed droplets from a laminar liquid jet. This approach enables the production of uniform macro- or microspheres. Moreover, utilizing coaxial nozzles, the prilling technique can create "core-shell" structures, providing a protective layer for sensitive biomolecules (Auriemma, Cerciello, et al., 2020; Del Gaudio et al., 2014). Therefore, the prilling technique is a suitable method for encapsulating compounds prone to oxidation. The choice of ingredients for the protective layer is crucial, and sodium alginate, a natural polymer, is an excellent option. Sodium alginate has shown very suitable properties for the encapsulation of several biomolecules, such as biocompatibility, gelation capability, versatile gel formation, selective permeability, stability, and biodegradability, which make it ideal for the protective layer both in the food and pharmaceutical field. The gelation of sodium alginate depends on divalent ions, such as calcium or zinc ions, which is a key functional property for its use in the food industry. The gelation process follows the classic egg-box model, in which two antiparallel polyuronate chains form egg-box dimers with divalent ions. These dimers then aggregate laterally, forming multimers, resulting in a stable and resilient shell (Cao et al., 2020; Hecht & Srebnik, 2016). To the best of our knowledge, omega-3-rich oils have never before been encapsulated with the prilling technique.

Encapsulation technologies are applied to protect omega-3 oils from oxidation but they also need to be available for absorption. Evaluations of the release of substances in the human digestive system require in vitro studies for which a standardized protocol with international consensus for the static simulation of human digestion is available (Brodkorb et al., 2019). In addition, the gastrointestinal tract has been recognized as a pro-oxidant environment due to low pH, presence of oxygen and metal ions. Also, the formation of micelles in the small intestine increases the exposure of to oxidants (Halliwell et al., 2000). Therefore, protection from oxidation must extend to the small intestine and oxidation should be followed from the ingestion to the digestive chyme to reveal the molecular species available for absorption. While the formation of secondary oxidation products during simulated digestion of cod liver, krill, and *Schizochytrium* sp oils has been recently monitored (Tullberg et al., 2019), no attention has been given to primary oxidation products nor to encapsulation of such oils in these conditions (Tullberg & Undeland, 2021).

The goal of the present work is to develop innovative high-load hydrophilic core soft-capsules based on alginate as carriers of DHA-rich *Schizochytrium* sp oil and to assess their oil release and protection from oxidation in a simulated gastrointestinal tract.

2. Materials and methods

2.1. Samples and reagents

Commercial oil from *Schizochytrium* sp was received as a donation. Sodium alginate M_W 160–190 KDalton was obtained from Carlo Erba SpA (Milan, Italy). Ultrapure water was prepared with Purelab Chorus instrument (Elga Veolia, High Wycombe, UK). All solvents were supplied by SigmaAldrich (Saint Luis, MO, USA) except deuterated DMSO, which was supplied by VWR (Leuven, Belgium), and MS-grade methanol and isopropanol, which were supplied by Honeywell/Riedel de Haën (Seelze, Germany). Regarding the salts utilized in this study, KCl, $MgCl_2$• 6 H_2O, NaOH, and HCl were supplied by VWR, KH_2PO_4 was supplied by Scharlau (Barcelona, Spain), $NaHCO_3$ was supplied by Avantor (Radnor, PA, USA), NaCl was supplied by Fischer Chemicals (Zürich, Switzerland), NH_4CO_3 was supplied by Merck (Darmstadt, Germany), and ammonium formate, $CaCl_2$• 2 H_2O, acetyl chloride, BHT, and heptadecanoic acid (17:0) were supplied by SigmaAldrich.

Rabbit gastric lipase (RGE15–500) was obtained from Lipolytech (Marseille, France). Amylase, porcine pepsin, porcine pancreatin, and bile salts were purchased from SigmaAldrich. Protease activity of pepsin was measured with the hemoglobin hydrolysis assay. Potato flour, whey protein concentrate, and wheat bran were supplied by Finnamyl Oy (Kokemäki, Finland), HSNG AB (Solna, Sweden), and Raisio Oy (Raisio, Finland), respectively.

2.2. Production of beads with prilling technique

For the manufacturing of core-shell microparticles, aqueous alginate solutions at different concentrations (between 1.00 and 2.00 %(*w/v*)) were used to form the shell of the gel beads. Alginate gel beads were prepared using a prilling apparatus (Encapsulator B-390, Büchi Labortechnik AG, St. Gallen, Switzerland), in coaxial configuration equipped with a 900 μm outer nozzle and 300 μm inner nozzle, and a double piston pump (Fusion 4000, Chemyx Inc., supplied by KR Analytical, Sandbach Cheshire, UK). Flow rate of each solution feeding the nozzles, as well as frequency of the vibration applied to the coaxial nozzle were set based on rheological properties of the feed solutions. Rheological analyses of feed solutions were conducted using an MCR 102 rheometer (Anton Paar GmbH, Graz, Austria) fitted with plate–plate geometry (PP25 with a diameter of 24.985 mm), selecting 1.5 mm as the measuring gap value and a shear rate from 0.1 to 100 (1/s) at 25 °C. The obtained gel beads were collected in aqueous solutions 0.5 M of $CaCl_2$ or Zinc acetate dihydrate placed at 8 cm from the nozzle exit. The collecting solutions were kept under gentle stirring for 10 min after the prilling process ended, and then the beads were washed with water. The process is summarized in **Supplementary Fig. 1**. Details about operating conditions are reported in **Supplementary Table 1**. The gel beads were air-dried or dried by means of a nitrogen flow (500 mbar) for 72 h. A 12-day storage trial was conducted to determine the effect of the bead drying flow (air or nitrogen) on the oxidation status of the encapsulated oil. Dried beads were stored for 6 and 12 days at 50 °C in duplicate and the tocopherol content of the oils (Section 2.7) utilized as oxidation marker.

2.3. Evaluation of size and shape properties

To evaluate the size of beads before and after drying as well as any variation either of the core or shell image analyses were conducted using ImageJ software (Wayne Rasband, National Institute of Health, Bethesda, MD, USA) and the software Axiovision (Carl Zeiss Vision, München-Hallbergmoos, Germany) on images collected by a fluorescence microscope Zeiss Axiophot (Carl Zeiss Vision, München-Hallbergmoos, Germany) equipped with a 20 × 1.4 NA no-oil immersion plan Apochroma objective, using standard optic filters. Fluorescein was added to the alginate solution as shell staining agent to enhance particle

analysis.

2.4. Oil content, surface oil, and encapsulation efficiency

The oil content of the beads was evaluated gravimetrically after extraction. Approximately 0.5 g of beads were homogenized in a tube with Ultraturrax homogenizer (IKA, Staufen, Germany) after addition of heptane. Isopropanol and 0.88 % KCl solution were added to the tube and homogenized again. The upper phase was recovered after vortexing for 30 s and centrifugation at 1610 × *g* for 3 min. The lower phase was extracted again, the upper phases combined and evaporated with nitrogen flow at 40 °C and the recovered oil weighed.

Surface oil was determined by washing 2 g of the soft capsules twice with 20 mL n-hexane and weighting the extracted lipids after evaporation of n-hexane (Takeungwongtrakul et al., 2015).

Encapsulation efficiency (EE) was calculated with the following equation

$$EE\ (\%) = \frac{Oil\ content - Surface\ oil}{Oil\ content} \times 100$$

2.5. Simulated digestion

2.5.1. Simulated meal

A simulated meal was prepared for the static in vitro digestion experiments. Potato flour, whey protein concentrate, and wheat bran were used as carbohydrate, protein, and fiber sources, respectively. The carbohydrate, protein, and fiber contents were calculated from the composition information provided by the manufacturers. The composition was calculated according to the energy intake of the simulated meal: 52.5 % of the energy derived from carbohydrates, 15 % derived from proteins, and 32.5 % derived from lipids. Fiber was added with the ratio 1 g/79.7 kcal of meal. Potato flour, whey protein, and wheat bran were defatted with exhaustive (48 h) Folch extraction (chloroform: methanol 2:1 *v/v*). The simulated meal was prepared by mixing the ingredients in the adequate ratios and heating at 100 °C for 20 min after addition of deionized water. Simulated meal and the lipid component were added separately (Beltrame et al., 2023).

2.5.2. Static in vitro digestion

The simulated in vitro digestion was performed according to the INFOGEST 2.0 protocol (Brodkorb et al., 2019) with modifications as reported previously (Beltrame et al., 2023). The whole procedure was carried out in dim light, while digestion itself was carried out in darkness. The compositions of simulated saliva, gastric fluid, and intestinal fluid were in accordance with the protocol. Enzyme solutions in their respective simulated fluids were prepared the day of the experiments. The required aliquots of $CaCl_2 \bullet 2\ H_2O$ 0.3 M were added to the simulated fluids only prior to enzyme addition. Solutions were preheated to 37 °C before use. The pH was adjusted with HCl and NaOH 1 M solutions. The required aliquots of HCl and NaOH solutions were verified prior to digestions.

Simulated oral phase. 0.90 g of simulated meal and 70 mg of neat or encapsulated oil were added with 1 mL of simulated saliva fluid, containing alfa-amylase 75 U/mL. The pH of the mixture was adjusted to 7. The chewing process was simulated with a clean glass rod by randomly hitting the mixture 32 times. Subsequently, mixture was incubated for 2 min at 37 °C.

Simulated gastric phase. The simulated oral bolus was added with 1 mL of simulated gastric fluid containing pepsin and rabbit gastric lipase to reach enzymatic activity of 2000 U/mL and 60 U/mL, respectively (final chyme volume). After pH adjustment to 3, the mixture was incubated for 2 h at 37 °C.

Simulated intestinal phase. The simulated gastric chyme was added with 2 mL of simulated intestinal fluid containing pancreatin and bile salts to reach concentrations in the digesta of 6 g/L (Versantvoort et al., 2005) and 10 mM, respectively. After pH adjustment to 7, the mixture was incubated for 2 h at 37 °C.

Blank digestions were performed following the same protocol in absence of oil.

2.5.3. Lipid extraction

Lipids were extracted immediately after digestion using hexane:isopropanol 2:1 *v*/v. The solvent contained BHT 0.05 % to prevent further oxidations. Throughout the procedure, samples were kept on ice. The solvent was added to the digestates in ratio 1:1 v/v and tubes were vortexed for 10 s and centrifuged at 1610 ×*g* for 3 min. The extraction was performed twice. Upper phases were combined and evaporated to dryness with N_2 at 37 °C. Samples were recovered with 3 mL of chloroform:methanol 1:1 and stored at −80 °C. Oil yield was measured gravimetrically and corrected with the extraction of blank digesta. Oil recovery was calculated from the known oil content of beads.

2.6. Fatty acid analysis

Fatty acids were methylated for GC analysis using methanolysis. Aliquotes of digestates, algal oil, and extracted bead oils were eventually dried, added with 2 mL of methanolic hydrochlorid acid mixture (prepared by adding acetyl chloride to methanol in 1:10 *v/v* ratio), and incubated overnight at 50 °C. Analysis was carried out with a Shimadzu GC-2030 equipped with autoinjector and FID. Heptadecanoic acid (17:0) was used as internal standard. Analytical details have been reported elsewhere (Damerau et al., 2020).

2.7. Tocopherol analysis

The concentrations of tocopherols in the different samples and digestates were analyzed with NP-HPLC-FLD, using a Shimadzu Nexera XR LC-30 system equipped with RF-20A fluorescence detector (292–325 nm excitation-emission wavelengths) and a Phenomenex OOG-4162-EO Luna 3 μm silica column (Aitta et al., 2023). A mixture of heptane and 1,4-dioxane (98:2) was used as mobile phase in isocratic mode. Column was kept at 30 °C, while the autosampler was kept at 4 °C. Tocopherol standard curves were prepared using α-, β-, γ-, and δ-tocopherol stock solutions.

Digestates were filtrated with 0.45 μm PTFE filters, dried with N_2 at room temperature in dim light and recovered with heptane. *Schizochytrium* sp oil was diluted in heptane. Oil extracted from beads was filtrated with 0.45 μm PTFE filters and diluted with heptane.

2.8. Analysis of digestion and non-volatile oxidation products

Digestion and non-volatile oxidation products were analyzed according to (Ahonen et al., 2022) with modifications. The analytical system consisted of Elute UHPLC and Bruker Impact II QTOF instruments from Bruker Daltonic (Bremen, Germany) equipped with Phenomenex (Torrance, CA, USA) Kinetex 2.6 μm PS C18 column (100 × 2.1 mm). Column and autosampler temperatures were 30 °C and 10 °C, respectively. Samples were diluted to 0.04 mg/mL in MeOH: chloroform (1:1). Injection volume was 1 μL. Binary mobile phase consisted of 95 % water, 5 % methanol, and 10 mM ammonium formate (Solvent A) and 70 % 2-propanol, 30 % methanol, 0.1 % water and 10 mM ammonium formate (Solvent B). The solvent gradient program was as follows: B increased from 60 % to 90 % in 3 min, to 96.5 % in 8 min, to 100 % in 0.5 min, held for 2 min, decreased to 60 % in 0.5 min and held for 3 min. Total run time was 18.5 min and flow rate 0.3 mL/min. Electrospray ionization (ESI) was applied in positive mode. The capillary voltage was set to 4.5 kV and end plate offset set to 500 V. Nebulizer gas pressure, drying gas flow rate, and drying gas temperature were 1.5 bar, 4 L/min, and 350 °C, respectively. Auto MS/MS scanning mode from 60 to 1200 *m/z* was applied. Internal calibration was performed with sodium formate. The concentration of the samples were equalized before

analysis. Peak area values were obtained with Bruker Compass DataAnalysis (Bruker Daltonic, Bremen, Germany).

2.9. ^1H NMR

^{1}H NMR spectra were collected from undigested lipid components and lipids extracted from digesta. For the analysis, 500 μL of sample were dried with N_2 flow and recollected with 200 μL of a mixture 5:1 of $CDCl_3$ and DMSO-d_6 (previously dried with 4 Å molecular sieves), of which 180 μL were pipetted in 3 mm NMR tubes. Samples were prepared the previous day of the analysis and stored overnight at −20 °C in desiccators. ^{1}H NMR spectra were collected at 298 K with a Bruker Avance 600 MHz equipped with a Prodigy TCI CryoProbe and SampleJet sample changer. Proton spectra were collected with 32 scans, acquisition time of 4 s, and relaxation time of 5 s. Selective gradient excitation pulse program (*selgpse*) was applied for region-specific excitation of hydroperoxide (11.5–10.5 ppm) and aldehyde (10–9 ppm) protons. The program had 128 scans, 4 dummy scans, acquisition time of 2.7 s, and relaxation time of 5 s. The 180-degree shaped pulse had a length of 1566.15 s (Ahonen et al., 2022). NMR data was processed with TopSpin 4.0.7 (Bruker, MA, USA) software.

2.10. Statistical analysis

The statistical analysis was performed with RStudio (RStudio, 2020). Shapiro-Wilk and Levene tests (*dlookr* and *car* packages) were used to assess normality of the data and homogeneity of data variance. The analysis of variance was performed with the functions *aov* and *TukeyHSD* (*stats* package) for ANOVA test or *oneway* for Games-Howell posthoc test (*userfriendlyscience* package). The confidence level of 95 % ($p < 0.05$) was used for statistical significance.

Principal component analysis (PCA) was performed with *FactoMineR* package. The most important loadings of the obtained PCA model were selected according to their cos2 values (*fviz_cos2* function of *factoextra* package). Variable correlations with principal components and their respective *p*-values were computed with *dimdesc* function (*FactoMineR* package).

Binning of NMR data was performed with *mrbin* package (Klein, 2021) using a bin width of 0.04 ppm and partial least squares-discriminant analysis (PLS-DA) was performed with *ropls* package (Thévenot et al., 2015) to discriminate undigested oils from digestate extracts.

3. Results and discussion

3.1. Optimization of the oil encapsulation process by prilling technique

The prilling output is influenced by the characteristics of the polymer solution, particularly viscosity, which is a critical factor in the feasibility of the process (Martinez et al., 2004). Therefore, during the optimization of the process, technical parameters such as vibration frequency, solution flow rates, and alginate concentration were adjusted to achieve satisfactory jet characteristics. Since this was the first time that such encapsulation technique was used to encapsulate *Schizochytrium* sp oil, a series of preliminary experiments were conducted to set various operating parameters to achieve beads of the desired size with a centered oil core. Detailed information about all the parameters used is provided in **Supplementary Table 1**. Specifically, alginate solutions (1.00–2.00 % *w/v* concentration) were used, which, in terms of viscosity, allowed a feasible production process (Rodríguez-Dorado et al., 2018). Initially, beads were produced utilizing a 1 % (*w/v*) solution and 1:1 ratio between the two flow rates to maximize the amount of oil contained in each bead. The resulting beads had proper size and consistency, but their core was mainly uncentered. In addition, oil leaking was also observed during the hardening process, probably due to the formation of an alginate layer too thin to act as a barrier to the diffusion of the oily core. Therefore, the flow rate of the polymeric solution was increased, until an optimal ratio of 4:1 was reached, allowing the production of gel beads with a well-defined core-shell architecture, desired size, and proper arrangement of the oily core. Specifically, inner core flow rate at 7 mL/min and flow rate to the outer nozzle of 28 mL/min produced beads with a diameter slightly above 1 mm. Such size granted easy handling and a proper amount of oil for each bead.

Two methods to remove the aqueous phase from the gel particles were tested in order to evaluate the effect of drying process on 1 % CaAlg bead properties, namely simple air exposure and nitrogen flow. The size of the beads was affected by drying method, with a size reduction more effective (around 10 %) in case of nitrogen based drying (Fig. 1). The drying method also affected stability of the encapsulated oil, with nitrogen-based method being capable to preserve more effectively oil components (Section 3.2). Further studies investigated the influence of alginate concentration (from 1.0 % to 2.0 % *w/v*) on beads mechanical strength and encapsulation process. At the highest concentration of alginate (2.00 % *w/v*), the nozzle vibration was barely able to cut the flow of the material coming out of the nozzle, leading to irregular particles in terms of size and shape, whereas with both 1.50 % and 1.75 % (*w/v*) alginate solution was possible to produce regular particles. Alginate 1.50 % w/v solution yielded regular beads with high oil content (**Supplementary Table 1**, batches 14 and 15) but, in order to grant the maximum mechanical resistance to the beads, alginate 1.75 % w/v was used for further experiments. Such beads, even though very promising in terms polymer/oil ratio, proved to be fragile after the drying process. For the production of 1.75 % CaAlg beads, vibrational frequency of 250 Hz and $CaCl_2$ concentration of 0.5 M n the gelling bath ensured narrow size distribution and spherical shape of beads. These values were the most suitable to achieve a clean cut of the laminar flow and quick gelation of the CaAlg beads. Additionally, since other divalent cations can quickly promote the gelation process of alginate (Auriemma, Russo, et al., 2020), the effect of Zn^{2+} on the core/shell beads was investigated using the same optimized operating parameters used for Ca^{2+} beads. Zinc was chosen not only for its gelling properties but also for its potential as a dietary supplement, given its essential role in various biological processes such as enzyme function and immune response (Prasad, 2013).

3.2. Size and morphological properties of the beads

The CaAlg beads were slightly larger in size than the ZnAlg beads, but they retained more water after the drying process, which led to a stronger reduction in size of the gel beads (Fig. 1 and Table 1). The size difference is due to the atomic radius of the cross-linking ions: calcium ions produce larger and more resistant beads than zinc ions. The water retention is related to the electron polarization of the cations: Zn^{2+} has a lower polarization than Ca^{2+}, which weakens its attraction to water molecules (Katz et al., 1996). Image analyses and fluorescence microscopy (Fig. 1) revealed the round shape, the core-shell structure, and the size variation of the gel beads before and after drying. The fluorescence images also showed that the shell of the 1.75 % Alg beads was thicker in the hydrated state, indicating a better encapsulation due to the higher alginate concentration. As expected, beads with a tougher polymeric layer due to the amount of alginate were able to reduce oil leaking both during beads formation and the drying process. Rheological analysis on solutions at different concentrations (Fig. 2) confirmed the direct relationship between concentration and viscosity, which can explain the different flow rates used in the prilling process. Moreover, higher concentrations showed a more pseudo-plastic behavior of the polymer solution leading to a more reproducible behavior at the nozzle, which facilitated the production of beads in narrow size distribution.

3.3. Oil content, encapsulation efficiency, and release

All beads showed an oil content between 80 and 95 % (Table 1),

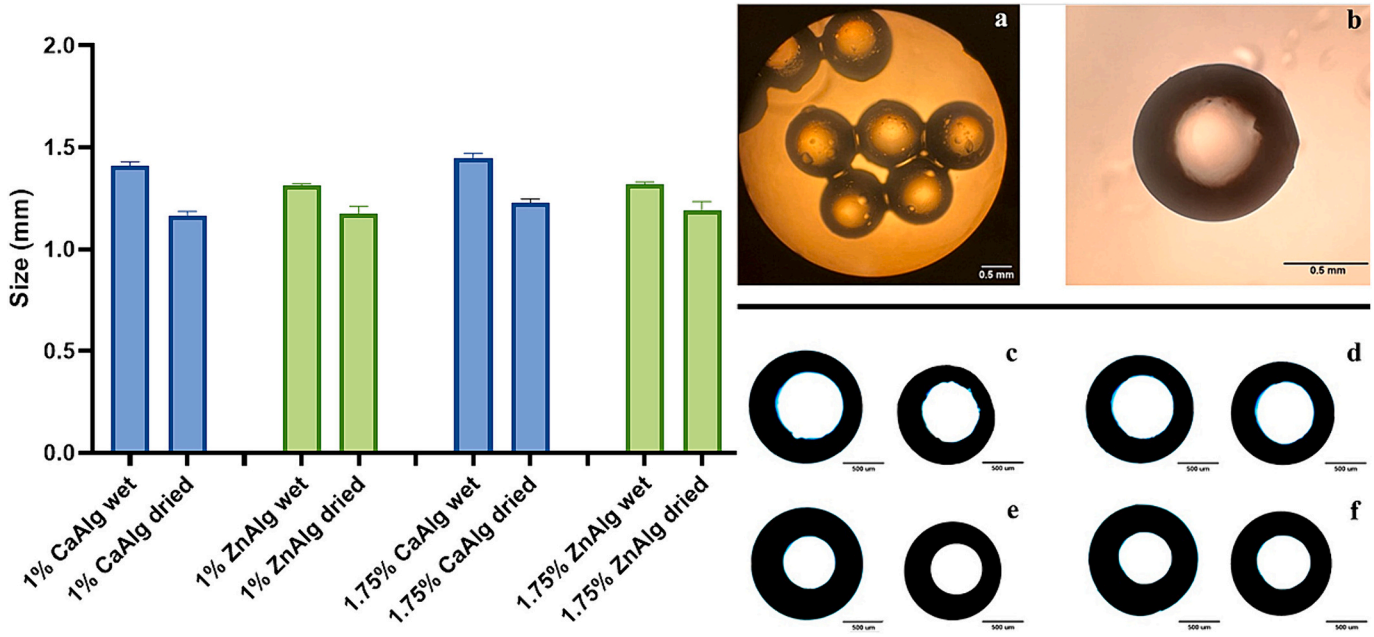

Fig. 1. Left: Beads size before and after nitrogen drying (mean values ± sd; $n = 3$). CaAlg beads are represented in blue and ZnAlg beads in green. Right**:** Optical microscopy images of 1.75 % CaAlg beads in hydrated (a) and dried state (b); fluorescence microscope (FM) images of wet and dry 1 % CaAlg (c), 1 % ZnAlg (d), 1.75 % CaAlg (e), and 1.75 % ZnAlg (f) beads, where alginate shells are labeled with fluorescein (in black) and cores result transparent (in white). (For interpretation of the references to colour in this figure legend, the reader is referred to the web version of this article.)

Table 1
Dimensional analyses and internal and surface oil content of produced beads (mean values ± sd; $n = 3$). Test samples have been analyzed only in their average diameter and oil content.

Bead	Core size (nm)	Shell size (nm)	Mean diameter (mm)	Oil content (%)	Surface oil (%)	EE (%)
1 % CaAlg air dried (test)	n.a.	n.a.	1.211 ± 0.12	82.7 ± 0.5a	n.a.	n.a.
1 % CaAlg N_2 dried (test)	n.a.	n.a.	1.109 ± 0.19	87.3 ± 0.8b	n.a.	n.a.
1 % CaAlg	0.703 ± 0.014	0.298 ± 0.007	1.163 ± 0.08	89.2 ± 2.5b	1.9 ± 0.1	97.8
1.75 % CaAlg	0.639 ± 0.011	0.337 ± 0.028	1.230 ± 0.17	94.9 ± 1.0b	19.0 ± 0.3	80.0
1 % ZnAlg	0.730 ± 0.023	0.287 ± 0.010	1.117 ± 0.23	82.1 ± 1.9a	57.0 ± 6.3	30.5
1.75 % ZnAlg	0.669 ± 0.008	0.312 ± 0.015	1.193 ± 0.41	83.4 ± 2.2a	28.2 ± 1.7	66.2

which is remarkably higher than conventional microbeads produced with spray-drying technique (Damerau, Mustonen, et al., 2022). Microencapsulation was recently considered a suitable method for the fortification of yogurt with *Schizochytrium* sp oil by Hyatt and coauthors, but oil content of microbeads was absent from their report (Hyatt et al., 2023). Compared to ours, their reported EEs (89.6 %–99 %) were similar or higher but they were achieved by double emulsion, which is more laborious than the prilling technique.

The increase in alginate concentration overall had a scant effect on the oil content of the beads. The beads containing zinc ions, compared to beads with calcium, had a lower oil load (82 % compared to 89 % and 83 % compared to 89 % for ion concentrations of 1 % and 1.75 %, respectively) and higher surface oil (57.0 against 1.9 and 28.2 against 19), which reflected in a clearly lower encapsulation efficiency. For this reason, and for the lower performance in the sensory evaluation studies (unpublished), zinc alginate beads were not submitted to simulated digestion studies.

Oil released at the end of the simulated digestion was extracted from the digesta, paying attention to integrity of the beads. Bead oil recovery was calculated from oil content (Table 1). Neat oil was digested for comparison. After simulated digestion, recovery of neat oil was almost quantitative (97.4 ± 0.5 %). The oil recovery observed with CaAlg 1.75 % was quantitative (89.5 ± 11.6 %). On the contrary, CaAlg 1 % had a recovery of 34.5 ± 10.6 %. It is known that coating affects oil release in simulated digestion. In the study of Annamalai, microcapsules of cod liver oil coated with maltodextrin and protein hydrolysate had lower release (68 %) compared to maltodextrin and sodium caseinate coating (75 %) (Annamalai et al., 2020). Fu and coworkers observed that *Schizochytrium* sp oil microencapsulated using whey protein or modified starch had different release profiles between gastric and intestinal phases but the same overall release (about 70 %) (Fu et al., 2020).

3.4. Fatty acid analysis and tocopherol content

Encapsulates were analyzed to verify the influence of prilling and gastrointestinal tract conditions on their fatty acid and tocopherol compositions. The main fatty acids and the tocopherol content of the *Schizochytrium* sp oil, the produced beads and their digestates are reported in Table 2. The fatty acid composition of the *Schizochytrium* sp oil (22:6n-3 remarkably almost 50 % *w/w* %) was in accordance with previous reports on thraustochytrid oils (Lee Chang et al., 2014). As observed in other thraustochytrids, 22:5n-6 was 8 % *w/w* %, 22:5n-3 almost absent (Table 2), and 20:5n-3 was only 1 % (not shown). The most abundant tocopherol was the γ-isomer (1781 ng/mg), followed by δ-tocopherol (691 ng/mg). Carotenoids were not investigated as the oil underwent refining.

Air and nitrogen flows were tested as drying agents for the beads at the end of the prilling process. The use of air had no statistically significant effect on the fatty acid or tocopherol composition of the bead oils. The concentration of γ-tocopherol in the air-dried beads was lower

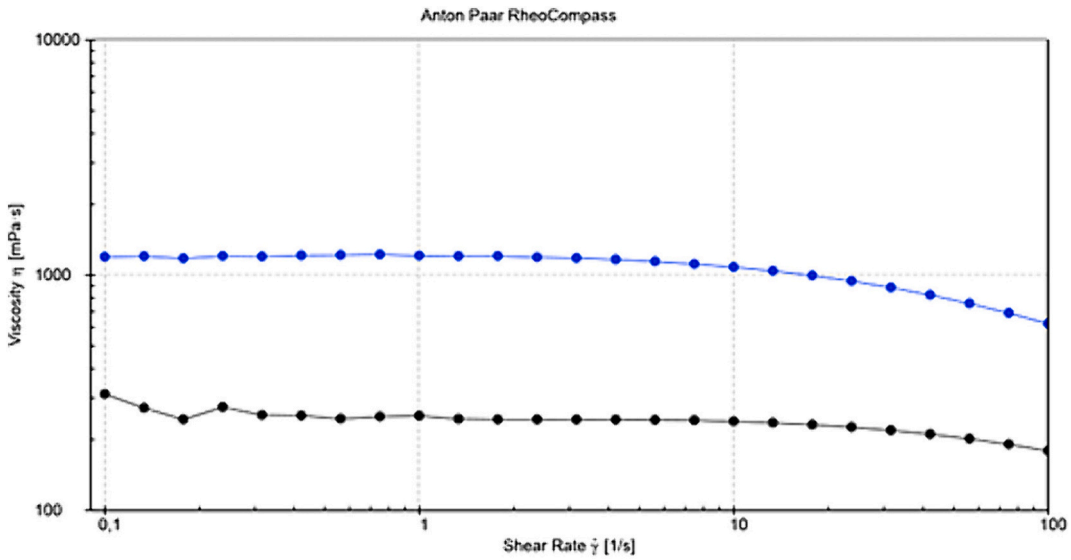

Fig. 2. Rotational rheological analysis of the two alginate solutions at different concentrations (1.75 % *w/v* in blue, 1 % *w/v* in black). (For interpretation of the references to colour in this figure legend, the reader is referred to the web version of this article.)

in comparison with the nitrogen-dried beads but it had no statistical significance (Table 2). On the other hand, remarkable differences were observed in a 12-days storage trial of the beads after test drying (**Supplementary Fig. 2**), after which nitrogen flow was selected for the final drying step in the production of all the subsequent batches.

Prilling had overall little influence on the fatty acid composition of the encapsulated oil. While no significant difference was observed after prilling with calcium, the utilization of zinc in the formulation of the beads had a limited but statistically significant negative effect on the 22:6n-3 and 22:5n-6 contents of the beads. At the same salt concentration, the content of these fatty acids decreased by about 6 % and 4 %, respectively. The overall PUFA decrease during manufacture of zinc beads was about 5 % (Table 2), further indicating calcium alginate as more promising coating agent. Conversely, prilling determined a decrease in the tocopherol content of the oil. Overall losses in γ-tocopherol ranged from 11 % (1 % CaAlg) to 19 % (1.75 % ZnAlg) and in δ-tocopherol from 13 % (1 % ZnAlg) to 22 % (1.75 % CaAlg). Losses in α-tocopherol were all around 10 %, while no significant loss in β-tocopherol was observed. The microencapsulation process utilized by Hyatt determined a loss in 22:6n-3 content of *Schizochytrium* sp oil of about 7 %, which increased to about 9 % oil when the oil was gelated prior to encapsulation (Hyatt et al., 2023). Such losses were counteracted by further addition of antioxidants, a step absent in the present work.

Losses in tocopherols were observed after simulated digestion but were significant mainly in unprotected oil. Significant losses of α-tocopherol were observed in unprotected and 1 % CaAlg oils (17 % and 15 % respectively) and losses of γ- and δ-tocopherol were observed only in the unprotected oil (14 % and 17 %, respectively). Statistically significant decreases in 22:5n-6, 22:6n-3, and PUFA relative contents were observed after simulated digestions of neat oil and calcium alginate beads. The losses of 22:5n-6 were around 9 %, 5 %, and 8 % for unprotected, 1 % CaAlg, and 1.75 % CaAlg, respectively, while the losses of 22:6n-3 were 10 %, 5 %, and 8 %, respectively. Therefore, in the present lab-scale experiments, the overall losses of PUFAs from refined oil to absorption in the small intestine were about 9 %, 4 %, and 7 % for unprotected, 1 % CaAlg, and 1.75 % CaAlg oils, respectively. Results would therefore indicate a tradeoff between reduction in the oxidative losses of PUFAs and bioavailability of the oil, as 1 % CaAlg beads had the lowest release (Section 3.2).

3.5. Non-volatile oxidation products and NMR analysis

Compound peak area data was obtained from the extracted ion chromatograms obtained from digesta of neat *Schizochytrium* sp oil and CaAlg beads. Non-volatile oxidation products of digesta were compared with undigested oils (neat and encapsulated) to verify the effect of simulated gastrointestinal tract on their formation and to verify whether encapsulation prevented their formation. A total of 41 compounds were identified as ammonium and sodium adducts. Different lipolysis products (DAGs and MAGs) were observed. Primary (hydroperoxidated, +2O) and secondary (hydroxylated or epoxidated, +1O) oxidation products were identified as M+32 and M+16, respectively. The oxygen additions were all observed with 22:6n-3 chains. Hydroperoxides produced fragments ascribable to different isomers, as 22:6n-3 contains multiple abstractable hydrogens and consequently different electron-deficient chain positions favoring reaction with oxygen (Schaich et al., 2013). These molecules were identified with the losses of 126 Da (14-OOH), 127 Da (16-OOH), 86 Da (17-OOH), 46 (20-OOH), and by the sodiated DHA + 32 (*m/z* 383.2) fragment. Secondary oxidation products were mainly identified with the sodiated DHA + 16 (*m/z* 367.2) fragment. **Supplementary Table 2** reports mass values (*m/z*) for the identified compounds and the main fragments used for identification, while **Supplementary Fig. 3** shows the peak area data of the identified compounds before and after digestion. Fig. 3 focuses on the peak area data of the oxidation products.

On average, the oxidation compound with highest area in neat oil was TAG 14:0/16:0/22:6 + 1O, while in encapsulated oils and all digestates the compound with highest area was TAG 16:0/22:6/22:6 + 2O. According to the HPLC-qTOF results, neat oil and oil encapsulated with 1.75 % CaAlg had a very similar oxidation profile. Prior to digestion, six oxidized TAGs out of seventeen oxidation products had statistically significantly higher area in 1 % CaAlg oil compared to the other two samples and one compound (DAG 18:1/22:6 + 2O) was observed only in 1 % CaAlg (Fig. 3). Therefore, 1.75 % CaAlg, despite its higher surface oil and lower encapsulation ratio, was oxidized less than 1 % CaAlg. Although surface oil was higher in 1.75 % CaAlg than 1 % CaAlg beads, the core size, the shell size, the mean diameter (Table 1), and the fluorescence microscope images (Figs. 1c,e) showed that the structure of 1.75 % CaAlg had a bigger wall size with less irregularities than 1 % CaAlg beads, which prevented oxidation of the encapsulated oil by delaying oxygen transfer to the oil core better than the 1 % CaAlg beads. As the core contained most of the bead oil, its oxidation status had a

Table 2
Major fatty acid composition and tocopherol content of neat and encapsulated *Schizochytrium* sp oil, including digestates. Different letters mark significant difference ($p < 0.05$).

	Fatty acid (w/w%)										Tocopherol (ng/mg)			
	14:0	16:0	16:1n-7	18:1n-9	22:5n-6	22:5n-3	22:6n-3	ΣSAFA	ΣMUFA	ΣPUFA	(n-3)/(n-6)	α	β	γ	δ
Neat oil	9.07 ± 0.01a	18.03 ± 0.01a	5.16 ± 0.02d	5.28 ± 0.01c	8.32 ± 0.02a	0.20 ± 0.02a	49.49 ± 0.03c	28.95 ± 0.03a	10.64 ± 0.04c	60.41 ± 0.06a	5.91 ± 0.01a	428.78 ± 12.83d	58.06 ± 1.92d	1781.13 ± 50.51c	690.61 ± 11.15b
1 % CaAlg air dried (test)	9.23 ± 0.02a,b	18.28 ± 0.01a	5.30 ± 0.01a,b	5.35 ± 0.01a	8.24 ± 0.01a	0.21 ± 0.01a	48.90 ± 0.01a	29.34 ± 0.02a	10.87 ± 0.01a	59.8 ± 0.02a	5.89 ± 0.01a	386.21 ± 20.94a,b	54.60 ± 7.22a,b,c	1558.75 ± 2.92a	566.41 ± 7.96a
1 % CaAlg N_2 dried (test)	9.24 ± 0.01a,b	18.28 ± 0.01a	5.31 ± 0.01a,b	5.35 ± 0.01a	8.22 ± 0.01a	0.22 ± 0.01a	48.87 ± 0.01a	29.37 ± 0.02a	10.85 ± 0.01a	59.78 ± 0.03a	5.90 ± 0.01a	372.95 ± 9.27a,b,d	57.61 ± 0.95a,b,c	1575.21 ± 11.09a	565.49 ± 4.56a
1 % CaAlg	9.12 ± 0.03a	18.13 ± 0.04a	5.17 ± 0.01b,d	5.30 ± 0.02c	8.30 ± 0.01a	0.24 ± 0.01a	49.19 ± 0.02a,c	29.16 ± 0.06a	10.66 ± 0.03c	60.18 ± 0.06a	5.88 ± 0.01a,d	379.5 ± 9.41a,b	58.28 ± 1.54b,c	1583.05 ± 41.87a	568.71 ± 16.12a
1.75 % CaAlg	9.10 ± 0.01a	18.10 ± 0.01a	5.16 ± 0.01d	5.28 ± 0.01c	8.31 ± 0.01a	0.22 ± 0.04a	49.36 ± 0.04a,c	29.05 ± 0.02a	10.64 ± 0.01c	60.31 ± 0.01a	5.88 ± 0.02a,d	370.96 ± 2.22a,b,d	59.91 ± 0.20b	1509.84 ± 17.60a,b	541.02 ± 5.48a
1 % ZnAlg	9.47 ± 0.09b,d	19.87 ± 0.09e	5.51 ± 0.04f,g	5.89 ± 0.02e	8.00 ± 0.01b,e	0.16 ± 0.03a	46.22 ± 0.18f	31.12 ± 0.26e	11.64 ± 0.07e,f	56.99 ± 0.28e	5.72 ± 0.02c,e	403.48 ± 10.30b,e	60.20 ± 1.83a,c,d	1530.41 ± 38.50a,b	598.39 ± 16.17a
1.75 % ZnAlg	9.39 ± 0.12b,d	19.86 ± 0.05e	5.42 ± 0.15a,g	5.90 ± 0.02e	8.05 ± 0.06e	0.19 ± 0.11a	46.35 ± 0.07b,f	31.13 ± 0.22e	11.53 ± 0.17f	57.22 ± 0.32b,e	5.70 ± 0.03e	383.55 ± 2.60a,b	55.89 ± 0.67a,b,c	1437.96 ± 11.84a,b	563.23 ± 5.28a
Neat oil (d)	9.50 ± 0.02d	21.28 ± 0.14d	5.64 ± 0.01e,f	5.68 ± 0.01d	7.55 ± 0.05d	0.20 ± 0.05a	44.74 ± 0.22e	33.00 ± 0.21d	11.8 ± 0.09d,e	55.2 ± 0.28d	5.78 ± 0.02b,c	355.24 ± 31.03a,c,d	58.79 ± 5.57a,b,c	1531.46 ± 135.26a,b	571.67 ± 52.42a
1 % CaAlg (d)	8.77 ± 0.23c	19.14 ± 0.46b	5.81 ± 0.01c	5.75 ± 0.04b	7.91 ± 0.08b	0.24 ± 0.04a	46.81 ± 0.45b	30.04 ± 0.65b	12.14 ± 0.07b	57.82 ± 0.58b	5.77 ± 0.03b,c	322.89 ± 11.75c	62.01 ± 3.74a,d	1422.52 ± 59.57a,b	596.58 ± 17.34a
1.75 % CaAlg (d)	9.42 ± 0.02b,d	20.58 ± 0.09c	5.75 ± 0.01c,e	5.75 ± 0.01b	7.67 ± 0.05c	0.25 ± 0.01a	45.35 ± 0.13d	32.2 ± 0.13c	11.86 ± 0.01d	55.94 ± 0.12c	5.82 ± 0.04b,d	336.57 ± 14.58c,d	57.18 ± 3.60a,b,c	1367.36 ± 89.86b	549.61 ± 40.98a

bigger impact on the overall status than the surface oil oxidation. After digestion, eleven species (seven TAGs and four DAGs) had significantly higher area in 1 % CaAlg compared to other samples (Fig. 3). Species with higher area compared to undigested samples were also eleven (four TAGs and all the seven DAGs). Of these, only the increases in DAG 22:6/22:6+2O and DAG 18:1/22:6+1O were observed in neat oil and still without significant difference with 1.75 % CaAlg oil. For the other nine species, the increases were observed in 1 % CaAlg. In four cases (TAG 14:0/22:6/22:6+1O, DAG 18:1/22:6+1O, DAG 16:0/22:6+1O, and DAG 14:0/22:6+1O), the increased area was not statistically significant compared to the other samples.

The cumulative areas of digestion and oxidation products identified with HPLC-qTOF are reported in **Supplementary Fig. 4**. The total area of digestion products in 1 % CaAlg digestates was significantly higher than 1.75 % CaAlg digestates, while difference with neat oil had no statistical significance. However, while the total DAG area followed the trend of total digestion products, total MAG area was higher in 1 % CaAlg digestate. In particular, the difference in area of MAG 22:6 (**Supplementary Fig. 2**) was statistically significant. The total area of oxidation products was higher in 1 % CaAlg digestate than both neat and 1.75 % CaAlg digestates but the difference prior to digestion lacked statistical significance. Oxidation of omega-3-rich oils after encapsulation is typically monitored with colorimetric rather than chromatographic methods. Nevertheless, some parallels can be drawn from the literature, as it is known that the oxidation degree caused by encapsulation depends on the coating material and process used and even modification of one parameter only may affect it. Annamalai observed that peroxide value of encapsulated cod liver oil increased only marginally from the value of neat oil when wall material contained protein hydrolysate rather than sodium caseinate (Annamalai et al., 2020). Aghbashlo et al. noticed that different wall materials increased the peroxide value of encapsulated fish oil differently, and milk protein had no significant effect (Aghbashlo et al., 2013). In the study of Fu et al., no significant increase in peroxide value was observed after microencapsulation of *Schizochytrium* sp oil using whey protein or modified starch (Fu et al., 2020). Lehn and coworkers, on the other hand, noticed that encapsulation of carp oil with whey protein-permeate blend almost doubled the peroxide value of the oil compared to the use of whey protein only (Lehn et al., 2018).

Scores and loading plots of the principal component analysis (PCA) of the HPLC-qTOF data of structured lipids are reported in Fig. 3a. The first principal component (PC1) separated digestates from undigested samples and represented more than 65 % of the data variance. In the score plot (Fig. 3a, left), undigested encapsulated oils positioned very closely on PC1, with the neat oil samples being closer to 1.75 % CaAlg beads. On the other hand, digestates of 1.75 % CaAlg beads grouped together in the lower right quadrant of the score plot, while digestates from 1 % CaAlg beads grouped together in the upper right quadrant. On both principal components, digestates from neat oil were positioned between the two encapsulated oils. Digestates of 1 % CaAlg beads had the highest score values on both PC1 and PC2. The loading plot (Fig. 3a, right) and the *p*-values of the loading correlation with PC1 and PC2 (Fig. 3b) show that discrimination on PC1 was determined mainly by eight digestion products (primarily MAG 14:0 and MAG 22:6, Fig. 3b) and two oxidized DAGs, DAG 18:1/22:6+1O and DAG 22:6/22:6+2O. Conversely, primary and secondary TAG oxidation products, such as TAG 16:0/22:6/22:6+1O, TAG 14:0/16:0/22:6+1O, TAG 14:0/16:0/22:6+2O, and TAG 14:0/22:6/22:6+2O, were the main determinants of PC2. The oxidized digestion product DAG 18:1/22:6+2O contributed to both principal components. The heatmap of the correlation coefficients between identified compounds and the first five PCs (**Supplementary Fig. 5**) corroborates the separation of the samples according to digestibility and oxidation on PC1 and PC2, respectively.

Nuclear magnetic resonance spectroscopy has been already applied for the simultaneous study of oxidation and digestion products in lipid digesta (Beltrame et al., 2023; Nieva-Echevarría et al., 2017). In this

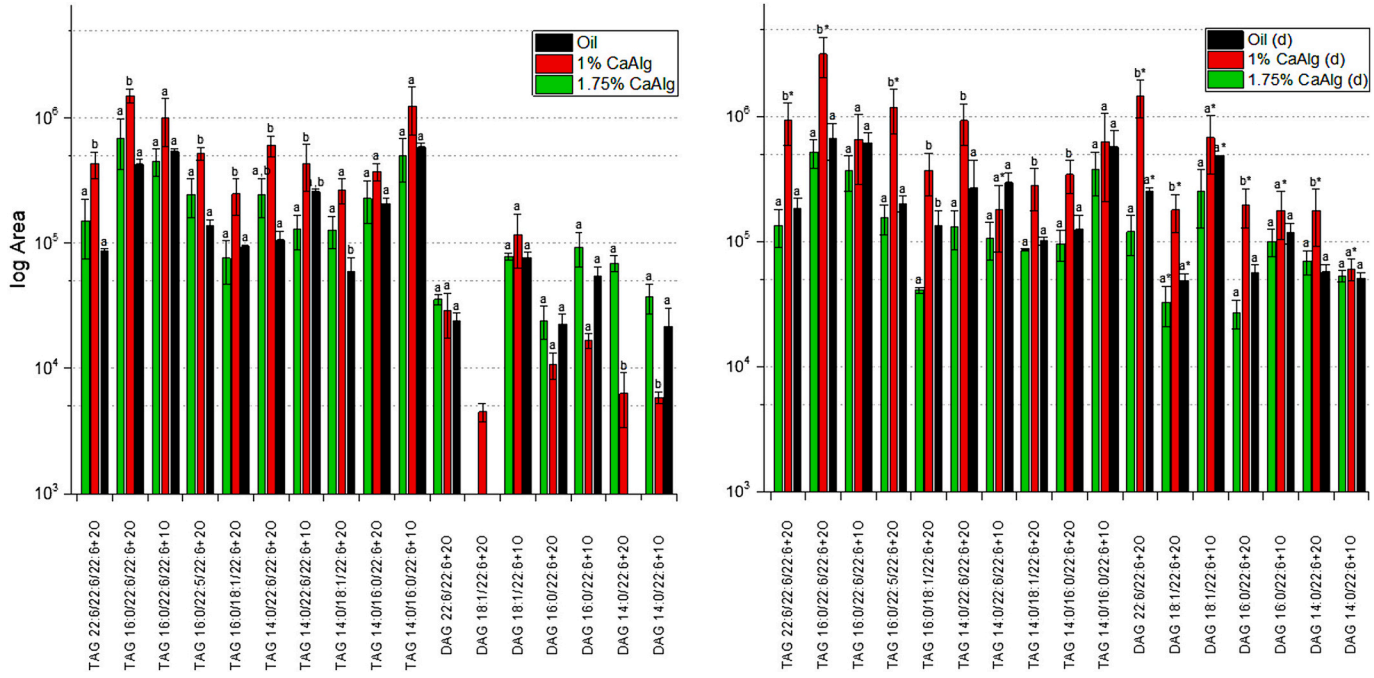

Fig. 3. Peak area values (in logarithmic scale) of non-volatile oxidation species identified in HPLC-qTOF chromatograms of neat and encapsulated *Schizochytrium* sp oil and their digestates (mean values ± sd; $n = 3$). Different letters mark significant difference ($p < 0.05$) in analyte area within sample class (undigested or digested). Asterisk marks significant difference ($p < 0.05$) between sample class (undigested vs digested).

work, a PLS-DA model was computed with binned ^{1}H NMR spectra. Its score and loading plots are reported in **Supplementary Fig. 6**. The model neatly discriminates undigested and digested samples. In the score plot, undigested beads grouped together and were separated from the neat oil, while digested oil was located between the two beads digesta, similarly to Fig. 4. According to the VIP scores, the bins which had highest correlation with undigested samples were 4.32 ppm, 4.16 ppm (both C*H*$_2$OR in TAGs), 2.32 ppm (C*H*$_2$-COOR in TAGs), and 0.88 ppm (saturated and n-9 terminal C*H*$_3$). On the other hand, digested samples were mainly discriminated by bins 3.68 ppm (2-MAG), 3.72 ppm (1,2-DAG), and 5.48 ppm (C*H*═C*H* associated with oxidation products) (Nieva-Echevarría et al., 2017). Therefore, spectroscopic data supported spectrometric data in indicating a correlation between oil release, lipolysis, and oxidation. The oil released by 1 % CaAlg was more oxidized than 1.75 % CaAlg but it had also more digestion products. The correlation of 1 % CaAlg with 2-MAG 22:6 is of high physiological importance, as this is the vector for the best absorption of this PUFA in the small intestine (Jin et al., 2020).

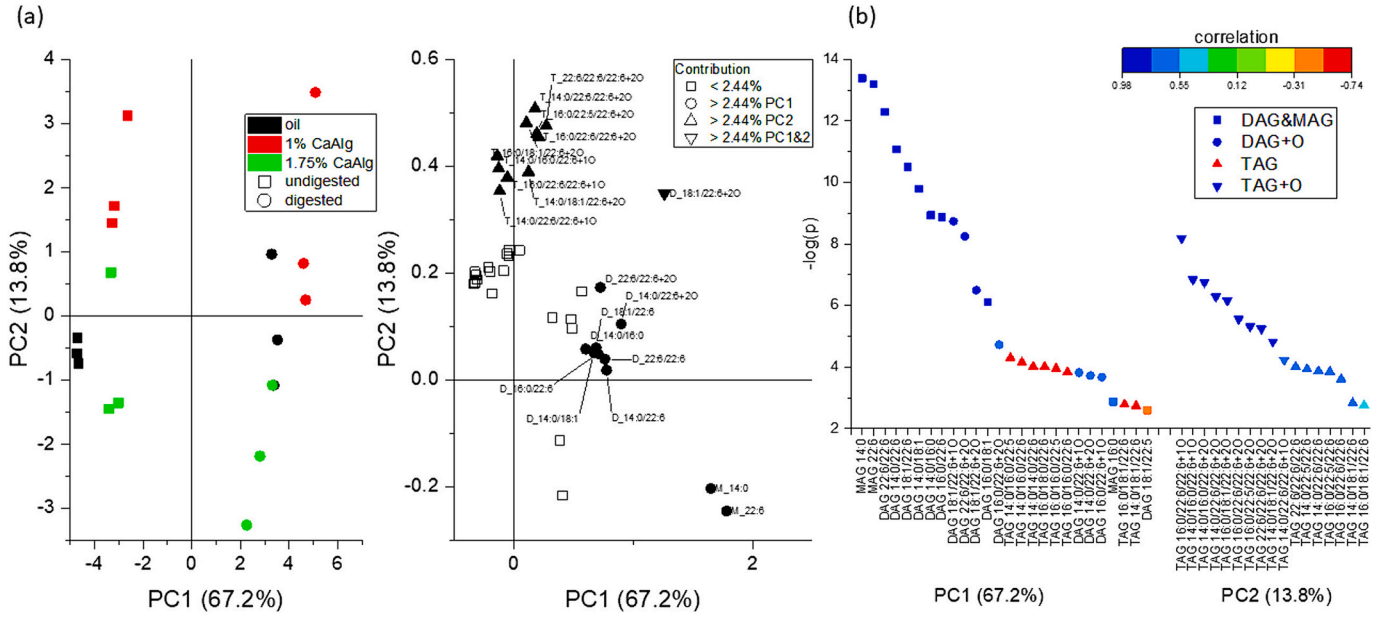

Fig. 4. Principal component analysis of HPLC-qTOF data of neat and encapsulated *Schizochytrium* sp oil and their digestates (a) and –log(*p*) of the correlation wih PC1 and PC2 of the most relevant lipid species for discrimination (b).

4. Conclusions

This study showed that the prilling technique was able to produce core/shell beads in narrow size distribution with *Schizochytrium* oil well centered in the core of the beads. The high load granted by prilling indicated that a low number of beads would be necessary to grant adequate dosages of 2-MAG 22:6n-3 to exert physiological effect. Encapsulation efficiency and fatty acid composition showed that calcium alginate was a better coating agent than zinc alginate. Gas chromatography showed no differences in PUFA content of encapsulates with the two calcium alginate formulas used (1 % and 1.75 %). HPLC-qTOF, on the other hand, showed higher presence of oxidation compounds in 1 % CaAlg prior to and after digestion, although only the latter was statistically significant. At the same time, the composition of 1 % CaAlg digestates showed higher amounts of digestion products. Further studies on the coating formulation are required to grant better protection from oxidation during production and to grant better release in the gastrointestinal tract.

Funding

A personal financial grant to Gabriele Beltrame from the Niemi Foundation is acknowledged. Personal financial grants to Annelie Damerau from the Finnish Cultural Foundation and to Eija Ahonen from the Niemi Foundation, the Finnish Cultural Foundation, and the Finnish Food Research Foundation are acknowledged. Personal financial grants to Sari A. Mustonen from the Turku University Foundation, the Finnish Cultural Foundation, and the Magnus Ehrnrooth foundation are acknowledged. This work was carried out as part of the project "Omics of oxidation-Solutions for better quality of docosahexaenoic and eicosapentaenoic acids" funded by the Academy of Finland (grant number 315274, PI Kaisa Linderborg).

CRediT authorship contribution statement

Gabriele Beltrame: Writing – original draft, Visualization, Investigation, Funding acquisition, Formal analysis. **Annelie Damerau:** Writing – review & editing, Methodology, Investigation, Conceptualization. **Eija Ahonen:** Writing – review & editing, Methodology. **Sari A. Mustonen:** Investigation. **Renata Adami:** Writing – review & editing. **Maria Rosaria Sellitto:** Investigation. **Pasquale Del Gaudio:** Writing – review & editing, Conceptualization. **Kaisa M. Linderborg:** Writing – review & editing, Supervision, Project administration, Funding acquisition, Conceptualization.

Declaration of competing interest

The authors declare that they have no known competing financial interests or personal relationships that could have appeared to influence the work reported in this paper.

Data availability

Data will be made available on request.

Acknowledgements

The authors would like to thank Iida Valta for her help in the GC-FID analysis, Enni Mannila for her help in the 12-days storage test, and Maaria Kortesniemi for her help in the NMR analysis.

Appendix A. Supplementary data

Supplementary data to this article can be found online at https://doi.org/10.1016/j.foodchem.2024.140694.

References

Aghbashlo, M., Mobli, H., Madadlou, A., & Rafiee, S. (2013). Influence of wall material and inlet drying air temperature on the microencapsulation of fish oil by spray drying. *Food and Bioprocess Technology, 6*(6), 1561–1569. https://doi.org/10.1007/s11947-012-0796-7

Ahonen, E., Damerau, A., Suomela, J.-P., Kortesniemi, M., & Linderborg, K. M. (2022). Oxidative stability, oxidation pattern and α-tocopherol response of docosahexaenoic acid (DHA, 22:6n–3)-containing triacylglycerols and ethyl esters. *Food Chemistry, 387*(March), Article 132882. https://doi.org/10.1016/j.foodchem.2022.132882

Aitta, E., Damerau, A., Marsol-Vall, A., Fabritius, M., Pajunen, L., Kortesniemi, M., & Yang, B. (2023). Enzyme-assisted aqueous extraction of fish oil from Baltic herring (Clupea harengus membras) with special reference to emulsion-formation, extraction efficiency, and composition of crude oil. *Food Chemistry, 424*, Article 136381. https://doi.org/10.1016/j.foodchem.2023.136381

Annamalai, J., Aliyamveetil Abubacker, Z., Lakshmi, N. M., & Unnikrishnan, P. (2020). Microencapsulation of fish oil using fish protein hydrolysate, Maltodextrin, and gum Arabic: Effect on structural and oxidative stability. *Journal of Aquatic Food Product Technology, 29*(3), 293–306. https://doi.org/10.1080/10498850.2020.1723765

Auriemma, G., Cerciello, A., Aquino, R. P., Del Gaudio, P., Fusco, B. M., & Russo, P. (2020). Pectin and zinc alginate: The right inner/outer polymer combination for Core-Shell drug delivery systems. *Pharmaceutics, 12*(2), 87. https://doi.org/10.3390/PHARMACEUTICS12020087

Auriemma, G., Russo, P., Del Gaudio, P., García-González, C. A., Landín, M., & Aquino, R. P. (2020). Technologies and formulation Design of Polysaccharide-Based Hydrogels for drug delivery. *Molecules, 25*(14), 3156. https://doi.org/10.3390/MOLECULES25143156

Beltrame, G., Ahonen, E., Damerau, A., Gudmundsson, H. G., Haraldsson, G. G., & Linderborg, K. M. (2023). Lipid structure influences the digestion and oxidation behavior of docosahexaenoic and Eicosapentaenoic acids in the simulated digestion system. *Journal of Agricultural and Food Chemistry, 71*(26), 10087–10096. https://doi.org/10.1021/acs.jafc.3c02207

Brodkorb, A., Egger, L., Alminger, M., Alvito, P., Assunção, R., Ballance, S., Bohn, T., Bourlieu-Lacanal, C., Boutrou, R., Carrière, F., Clemente, A., Corredig, M., Dupont, D., Dufour, C., Edwards, C., Golding, M., Karakaya, S., Kirkhus, B., Le Feunteun, S., & Recio, I. (2019). INFOGEST static in vitro simulation of gastrointestinal food digestion. *Nature Protocols, 14*(4), 991–1014. https://doi.org/10.1038/s41596-018-0119-1

Cao, L., Lu, W., Mata, A., Nishinari, K., & Fang, Y. (2020). Egg-box model-based gelation of alginate and pectin: A review. *Carbohydrate Polymers, 242*, Article 116389. https://doi.org/10.1016/J.CARBPOL.2020.116389

Colombo, S. M., Rodgers, T. F. M., Diamond, M. L., Bazinet, R. P., & Arts, M. T. (2020). Projected declines in global DHA availability for human consumption as a result of global warming. *Ambio, 49*(4), 865–880. https://doi.org/10.1007/s13280-019-01234-6

Damerau, A., Ahonen, E., Kortesniemi, M., Puganen, A., Tarvainen, M., & Linderborg, K. M. (2020). Evaluation of the composition and oxidative status of omega-3 fatty acid supplements on the Finnish market using NMR and SPME-GC–MS in comparison with conventional methods. *Food Chemistry, 330*(June), Article 127194. https://doi.org/10.1016/j.foodchem.2020.127194

Damerau, A., Mustonen, S. A., Ogrodowska, D., Varjotie, L., Brandt, W., Laaksonen, O., … Linderborg, K. M. (2022). Food fortification using spray-dried emulsions of fish oil produced with Maltodextrin, plant and whey proteins—Effect on sensory perception, Volatiles and Storage Stability. *Molecules, 27*(11), 3553. https://doi.org/10.3390/molecules27113553

Damerau, A., Ogrodowska, D., Banaszczyk, P., Dajnowiec, F., Tańska, M., & Linderborg, K. M. (2022). Baltic herring (Clupea harengus membras) oil encapsulation by spray drying using a rice and whey protein blend as a coating material. *Journal of Food Engineering, 314*, Article 110769. https://doi.org/10.1016/j.jfoodeng.2021.110769

Del Gaudio, P., Auriemma, G., Russo, P., Mencherini, T., Campiglia, P., Stigliani, M., & Aquino, R. P. (2014). Novel co-axial prilling technique for the development of core–shell particles as delayed drug delivery systems. *European Journal of Pharmaceutics and Biopharmaceutics, 87*(3), 541–547. https://doi.org/10.1016/J.EJPB.2014.02.010

Del Gaudio, P., Colombo, P., Colombo, G., Russo, P., & Sonvico, F. (2005). Mechanisms of formation and disintegration of alginate beads obtained by prilling. *International Journal of Pharmaceutics, 302*(1–2), 1–9. https://doi.org/10.1016/J.IJPHARM.2005.05.041

Demets, R., & Foubert, I. (2021). Traditional and novel sources of long-chain omega-3 fatty acids. In *Omega-3 Delivery Systems* (pp. 3–23). Elsevier. https://doi.org/10.1016/B978-0-12-821391-9.00013-2.

Fu, J., Song, L., Liu, Y., Bai, C., Zhou, D., Zhu, B., & Wang, T. (2020). Improving oxidative stability and release behavior of docosahexaenoic acid algae oil by microencapsulation. *Journal of the Science of Food and Agriculture, 100*(6), 2774–2781. https://doi.org/10.1002/jsfa.10309

Halliwell, B., Zhao, K., & Whiteman, M. (2000). The gastrointestinal tract: A major site of antioxidant action? *Free Radical Research, 33*(6), 819–830. https://doi.org/10.1080/10715760000301341

Hamilton, H. A., Newton, R., Auchterlonie, N. A., & Müller, D. B. (2020). Systems approach to quantify the global omega-3 fatty acid cycle. *Nature Food, 1*(1), 59–62. https://doi.org/10.1038/s43016-019-0006-0

Hecht, H., & Srebnik, S. (2016). Structural characterization of sodium alginate and calcium alginate. *Biomacromolecules, 17*(6), 2160–2167. https://doi.org/10.1021/ACS.BIOMAC.6B00378/ASSET/IMAGES/MEDIUM/BM-2016-00378B_0012.GIF

Hyatt, J. R., Zhang, S., & Akoh, C. C. (2023). Combining antioxidants and processing techniques to improve oxidative stability of a Schizochytrium algal oil ingredient with application in yogurt. *Food Chemistry, 417*. https://doi.org/10.1016/j.foodchem.2023.135835

Jin, J., Jin, Q., Wang, X., & Akoh, C. C. (2020). High Sn-2 docosahexaenoic acid lipids for brain benefits, and their enzymatic syntheses: A review. *Engineering, 6*(4), 424–431. https://doi.org/10.1016/j.eng.2020.02.009

Katz, A. K., Glusker, J. P., Beebe, S. A., & Bock, C. W. (1996). Calcium ion coordination: A comparison with that of beryllium, magnesium, and zinc. *Journal of the American Chemical Society, 118*(24), 5752–5763. https://doi.org/10.1021/JA953943I/SUPPL_FILE/JA5752A.PDF

Klein, M. S. (2021). Affine transformation of negative values for NMR metabolomics using the mrbin R package. *Journal of Proteome Research, 20*(2), 1397–1404. https://doi.org/10.1021/acs.jproteome.0c00684

Lee Chang, K. J., Nichols, C. M., Blackburn, S. I., Dunstan, G. A., Koutoulis, A., & Nichols, P. D. (2014). Comparison of Thraustochytrids Aurantiochytrium sp., Schizochytrium sp., Thraustochytrium sp., and Ulkenia sp. for production of biodiesel, long-chain Omega-3 oils, and exopolysaccharide. *Marine Biotechnology, 16*(4), 396–411. https://doi.org/10.1007/S10126-014-9560-5/FIGURES/6

Lehn, D. N., Esquerdo, V. M., Dahlem Júnior, M. A., Dall'Agnol, W., dos Santos, A. C. F., de Souza, C. F. V., & de Almeida Pinto, L. A. (2018). Microencapsulation of different oils rich in unsaturated fatty acids using dairy industry waste. *Journal of Cleaner Production, 196*, 665–673. https://doi.org/10.1016/j.jclepro.2018.06.127

Martinez, L., Agnely, F., Bettini, R., Besnard, M., Colombo, P., & Couarraze, G. (2004). Preparation and characterization of chitosan based micro networks: Transposition to a prilling process. *Journal of Applied Polymer Science, 93*(6), 2550–2558. https://doi.org/10.1002/APP.20785

Micha, R., Khatibzadeh, S., Shi, P., Fahimi, S., Lim, S., Andrews, K. G., … Mozaffarian, D. (2014). Global, regional, and national consumption levels of dietary fats and oils in 1990 and 2010: A systematic analysis including 266 country-specific nutrition surveys. *The BMJ, 348*(April), 1–20. https://doi.org/10.1136/bmj.g2272

Nieva-Echevarría, B., Goicoechea, E., & Guillén, M. D. (2017). Polyunsaturated lipids and vitamin A oxidation during cod liver oil in vitro gastrointestinal digestion. Antioxidant effect of added BHT. *Food Chemistry, 232*, 733–743. https://doi.org/10.1016/J.FOODCHEM.2017.04.057

Ortiz Sánchez, C. A., Zavaleta, E. B., García, G. R. U., Solano, G. L., & Díaz, M. P. R. (2021). Krill oil microencapsulation: Antioxidant activity, astaxanthin retention, encapsulation efficiency, fatty acids profile, in vitro bioaccessibility and storage stability. *LWT, 147*, Article 111476. https://doi.org/10.1016/J.LWT.2021.111476

Prasad, A. S. (2013). Discovery of human zinc deficiency: Its impact on human health and disease. *Advances in Nutrition, 4*(2), 176–190. https://doi.org/10.3945/an.112.003210

Rodríguez-Dorado, R., Landín, M., Altai, A., Russo, P., Aquino, R. P., & Del Gaudio, P. (2018). A novel method for the production of core-shell microparticles by inverse gelation optimized with artificial intelligent tools. *International Journal of Pharmaceutics, 538*(1–2), 97–104. https://doi.org/10.1016/J.IJPHARM.2018.01.023

RStudio. (2020). *RStudio: Integrated development for R*. Boston, MA: RStudio, Inc.. URL http://www.rstudio.com/.

Saini, R. K., & Keum, Y. S. (2018). Omega-3 and omega-6 polyunsaturated fatty acids: Dietary sources, metabolism, and significance — A review. *Life Sciences, 203*(January), 255–267. https://doi.org/10.1016/j.lfs.2018.04.049

Schaich, K. M., Shahidi, F., Zhong, Y., & Eskin, N. A. M. (2013). Lipid oxidation. In *Biochemistry of foods* (pp. 419–478). Elsevier. https://doi.org/10.1016/B978-0-08-091809-9.00011-X.

Schwarz, K., & Amft, J. (2021). Spray-dried capsules and extrudates as omega-3 lipids delivery systems. In *Omega-3 Delivery Systems* (pp. 321–343). Elsevier. https://doi.org/10.1016/B978-0-12-821391-9.00007-7.

Serini, S., Fasano, E., Piccioni, E., Cittadini, A. R. M., & Calviello, G. (2011). Dietary n-3 polyunsaturated fatty acids and the paradox of their health benefits and potential harmful effects. *Chemical Research in Toxicology, 24*(12), 2093–2105. https://doi.org/10.1021/tx200314p

Takeungwongtrakul, S., Benjakul, S., & H-kittikun, A. (2015). Wall materials and the presence of antioxidants influence encapsulation efficiency and oxidative stability of micro-encapsulated shrimp oil. *European Journal of Lipid Science and Technology, 117*(4), 450–459. https://doi.org/10.1002/EJLT.201400235

Thévenot, E. A., Roux, A., Xu, Y., Ezan, E., & Junot, C. (2015). Analysis of the human adult urinary metabolome variations with age, body mass index, and gender by implementing a comprehensive workflow for univariate and OPLS statistical analyses. *Journal of Proteome Research, 14*(8), 3322–3335. https://doi.org/10.1021/ACS.JPROTEOME.5B00354/SUPPL_FILE/PR5B00354_SI_003.ZIP

Tocher, D. R. (2015). Omega-3 long-chain polyunsaturated fatty acids and aquaculture in perspective. *Aquaculture, 449*, 94–107. https://doi.org/10.1016/j.aquaculture.2015.01.010

Tullberg, C., & Undeland, I. (2021). Oxidative stability during digestion. In *Omega-3 Delivery Systems* (pp. 449–479). Elsevier. https://doi.org/10.1016/B978-0-12-821391-9.00008-9.

Tullberg, C., Vegarud, G., & Undeland, I. (2019). Oxidation of marine oils during in vitro gastrointestinal digestion with human digestive fluids – Role of oil origin, added tocopherols and lipolytic activity. *Food Chemistry, 270*(May 2018), 527–537. https://doi.org/10.1016/j.foodchem.2018.07.049

Versantvoort, C. H. M., Oomen, A. G., Van De Kamp, E., Rompelberg, C. J. M., & Sips, A. J. A. M. (2005). Applicability of an in vitro digestion model in assessing the bioaccessibility of mycotoxins from food. *Food and Chemical Toxicology, 43*(1), 31–40. https://doi.org/10.1016/j.fct.2004.08.007